Journal of Membrane Science and Research 1 (2015) 118-123

Journal of Membrane Science and Research

journal homepage: www.msrjournal.com

Research Paper

Fabrication and Characterization of Polyetherimide Hollow Fiber Membrane Contactor for Carbon Dioxide Stripping from Monoethanolamine Solution

Zabih A. Tarsa[1], S. Ali Asghar Hedayat[1], Masoud Rahbari-Sisakht[2,*]

[1] *Chemical Engineering Department, Mahshahr branch, Islamic Azad University, Mahshahr, Iran*
[2] *Chemical Engineering Department, Gachsaran branch, Islamic Azad University, Gachsaran, Iran*

HIGHLIGHTS

- PEI HFM were fabricated using different amounts of ethanol.
- Membranes were used for CO_2 stripping from MEA solution.
- Fabricated membrane using 2.wt% ethanol showed higher stripping flux.

GRAPHICAL ABSTRACT

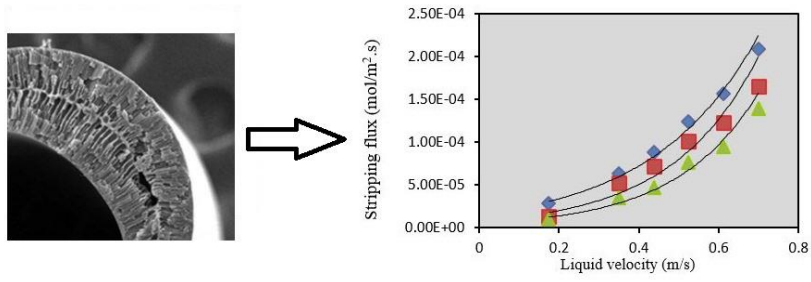

ARTICLE INFO

Article history:
Received 2015-02-14
Revised 2015-04-12
Accepted 2015-04-19
Available online 2015-04-19

Keywords:
Gas-liquid membrane contactor
CO_2 stripping
Hollow fiber membrane
Polyetherimide

ABSTRACT

In this research, process asymmetric polyetherimide hollow fiber membranes using ethanol (0, 2 and 4 wt%) as non-solvent additive in the polymer dope via phase inversion method were fabricated. Aqueous solution of 1-methyl-2-pyrrolidine (NMP) (90%) was applied as a bore fluid to avoid inner skin layer formation and water was used as the external coagulant. The morphology of fabricated membranes was examined using field emission scanning electron microscope (FESEM). A gas permeation test was conducted using Nitrogen. Fabricated membranes were characterized in terms of pore size, critical water entry pressure, water contact angle and collapsing pressure. The performance of fabricated membranes for carbon dioxide stripping from monoethanolamine solution using a gas - liquid membrane contactor system was studied. The results showed that carbon dioxide stripping flux and efficiency increased by increasing liquid velocity. Also, enhancement of stripping flux by increasing gas velocity was negligible. By increasing MEA solution temperature, stripping flux increased; therefore, liquid phase temperature is a key parameter which needs to be controlled.

© 2015 MPRL. All rights reserved.

1. Introduction

Most of the energy in the world comes from fossil fuels, such as coal, oil and gas. However, the combustion of fossil fuels inevitably results in the emission of air pollutants and a huge release of carbon dioxide. Since CO2 is a major greenhouse gas, it should be removed from industrial flue gas streams.

Many methods exist to remove CO_2 by absorption into aqueous solution of alkanolamines using conventional equipment including packed columns, bubble columns, and spray columns. The use of aqueous alkanolamines allows regeneration of the liquid absorbents by simple heating. Therefore, a

* Corresponding author at: Tel: +989173430307
E-mail address: rahbari@iaug.ac.ir (M. Rahbari-Sisakht)

typical process for CO_2 capture consists of two major units, absorption and desorption. Desorption is commonly carried out by using conventional columns that have operational problems such as flooding, channeling, and entrainment [1,2].

Hollow fiber membrane contactors for CO_2 capture have been studied over the past few decades [3,4]. Surprisingly, several studies have shown that hydrophilic polymer such as polyetherimide (PEI) polymers [5] that have been diversely used in ultrafiltration [6,7] and gas separation [8,9] can also be potentially applied in the membrane contactor due to its high wetting pressure and high absorption flux performance [10].

The structure of a membrane is influenced by the rate of the phase inversion process. The thermodynamic stability of the polymer solution and the diffusion rate of coagulant into the polymer solution are two important parameters that determine the rate of the phase inversion process, which further depends on the composition of the spinning dope and coagulation media [10]. A rapid phase inversion process forms finger-like macro-voids in the structure of the membrane and a slow phase inversion makes a sponge-like structure [11,12]. One method to alter the rate of the phase inversion process is blending additives to the spinning dope and/or coagulant. Polymers [13–15], non-solvents [16–18] and salts [19] are additives for spinning dope whereas solvents [20] and weaker non-solvents [21,22] are used as additive for coagulant.

The structure of the membrane also depends on the polymer concentration at the cloud point. Furthermore, highly water soluble phase inversion promoters of low molecular weight can be washed out during the phase inversion process, which in turn increases the porosity of the membrane [10].

Several reports have been published on CO_2 capture and stripping using hollow fiber membrane contactor, which were fabricated using different polymers. Rahbari-Sisakht et al. [23], polysulfone (PSf) HFM was produced and applied for CO_2 stripping from water. Results showed that liquid velocity and temperature are two important factors for the gas stripping process while, gas velocity has no significant effect.

Mansourizadeh and Ismail [24] studied the effects of different additives such as polyethylene glycol of average molecular weight of 200 Daltons (PEG200), glycerol, acetic acid and ethanol on the polysulfone (PSf) membrane morphology. Their results showed that adding glycerol into the spinning dope provided the membrane structure with a thin finger-like and a thick sponge-like layer, which resulted in a higher critical water entry pressure (CEPw) and CO_2 absorption rate than the other PSf hollow fiber membranes.

Bakeri et al. [10] added low molecular weight organic compounds to the spinning dope as phase inversion promoters and studied their effects on the structure of polyetherimide (PEI) hollow fibers. They employed water, methanol, ethanol, glycerol and acetic acid as additives in the spinning dope and fabricated hollow fiber membranes via the wet spinning method. Their results showed that the solution containing water as additive had the lowest thermodynamic stability and highest viscosity, which yielded a hollow fiber with a thin skin layer of high porosity and a sublayer with sponge-like structure. The four other polymer solutions were more stable thermodynamically and less viscous. Among all their fellow fiber membranes, adding methanol resulted in the highest absorption flux.

PEI is a polymer with good thermal and chemical stability that makes it a suitable candidate for contactor applications. In addition, the low viscosity and hydrophobicity of PEI solution promotes the formation of finger-like macrovoids in the structure of PEI membranes that decreases the membrane mass transfer resistance. Most studies on the effect of phase inversion promoters on the structure of PEI membranes were devoted to gas separation membranes, in which a dense skin layer should be present at the membrane surface. Research about the effect of low molecular weight additives on the structure and performance of porous PEI hollow fiber membranes in contactor applications is rare.

In this work, the membrane contactor based regeneration unit was developed to study the effect of some operating conditions such as the liquid and gas velocities and liquid phase temperature on the CO_2 stripping from monoethanolamine (MEA).

2. Experimental

2.1. Materials

Polyetherimide (PEI, Ultem®) was used for fabrication of the hollow fiber membranes. 1-Methyl-2-pyrrolidone (NMP, >99.5%) was supplied by Merck and used as solvent without further purification. Ethanol was purchased from Merck (Germany) and used as non-solvent additive in the polymer dopes. Tap water was used as coagulation bath in all cases. Monoethanolamine (MEA) (>98%) was supplied by SIGMA-ALDRICH and used as liquid absorbent.

2.2. Fabrication of PEI hollow fiber membranes

The PEI in pellet form was dried at 70±2 ºC in a vacuum oven for 24 h to remove the moisture. The spinning dopes of 18wt.% PEI, 2 and 4wt.% Ethanolin NMP were prepared by stirring the solution at room temperature until the solution became homogeneous. The resulting solutions were degassed for 24 h at room temperature before spinning. The hollow fiber spinning process by the wet phase inversion was described elsewhere [25]. Table 1 lists the detailed spinning parameters. The spun hollow fibers were immersed in water for 3 days to remove the residual NMP and Ethanol. Then, they were dried at room temperature.

Table 1
Spinning conditions of PEI hollow fiber membranes.

Dope extrusion rate (ml/min)	4.50
Bore fluid composition (wt%)	NMP/water 90:10
Bore fluid flow rate (ml/min)	2
External coagulant	Tap water
Air gap distance (cm)	0.0
Spinneret o.d/i.d (mm)	1.0/0.50
Coagulation temperature (ºC)	25

2.3. Field emission scanning electron microscopy (FESEM)

Field emission scanning electron microscopy (FESEM) (ZEIZZ SUPRA 35VP) was used to observe the morphology of the fabricated PEI hollow fiber membranes. The membrane samples were carefully fractured in liquid nitrogen to have a clean brittle fracture. Then, the samples were dried in a vacuum oven and coated by sputtering platinum before testing. The FESEM micrographs of the cross-section of the hollow fiber membranes were taken at various magnifications.

2.4. Gas permeation test

For a porous asymmetric membrane, the determination of pore size and particularly surface porosity is very important in studying mass transfer in the membrane gas absorption [26]. The total gas permeation through the asymmetric porous membrane is considered as the combination of the Poiseuille flow and Knudsen flow [27]. Li et al. [28] introduced a modified gas permeation method to determine the average pore size and the effective surface porosity over the effective pore length of the asymmetric membrane. By assuming cylindrical pores in the skin layer of the asymmetric membranes, the gas permeance can be given as:

$$J_i = \frac{2r_p\varepsilon}{3RTL_p}\left(\frac{8RT}{\pi M}\right)^{0.5} + \frac{{r_p}^2\varepsilon}{8\mu_i RTL_p}\bar{P} \text{ or } J_i = K_0 + P_0\bar{P} \quad (1)$$

By plotting J_i versus mean pressures according to Eq. (1), the average pore size can be calculated from the intercept (K_0) and slope (P_0) as follows:

$$r_p = 5.333\left(\frac{P_0}{K_0}\right)\left(\frac{8RT}{\pi M}\right)^{0.5}\mu_i \quad (2)$$

The effective surface porosity over pore length, ε/L_p, can also be obtained from the slope as:

$$\frac{\varepsilon}{L_p} = \frac{8\mu_i RTP_0}{r_p^2} \quad (3)$$

The test apparatus was based on the volume displacement method. The test module containing two hollow fibers with a length of 10 cm was used to determine gas permeability by shell side feed. The upstream pressure was in a range from 1×10^5 to 4×10^5 Pa (from 1 to 4 bar) (absolute). Pure N_2 was used as the test gas and its permeation rate was measured at 25 ◦C using a soap-bubble flow meter connected to the lumen side of the hollow fibers. The gas permeance test was conducted five times for each pressure and the average of the measured times was used for calculation based on the outer diameter of the hollow fiber.

2.5. Critical entry pressure of water, overall porosity and Collapsing pressure measurements

The test module similar to the one used in the gas permeation test was used to measure the critical entry pressure of water (CEPw). Distilled water was pumped into the lumen side of the hollow fibers. The pressure was gradually increased at a 0.5×10^5 Pa (0.5 bar) interval. At each pressure, the membrane module was kept at constant pressure for 30 min to check if any water droplet appeared in the outer surface of the fiber. The critical water entry pressure is the pressure at which the first water droplet appears on the outer surface of the hollow fiber.

The membrane overall porosity, ε_m, was determined by the gravimetric method. It is defined as the volume of the pores divided by the total volume of the membrane calculated by [28]:

$$\varepsilon_m = \frac{(w_1-w_2)/\rho_w}{(w_1-w_2)/\rho_w+w_2/\rho_p} \quad (4)$$

where w_1 is the weight of the wet membrane, w_2 the weight of the dry membrane, ρ_w water density and ρ_p the polymer density. In order to prepare the wet membranes, five spun hollow fibers were selected after 3 days solvent exchange with tap water. The fibers were immersed in distilled water for another 24 h and the remaining water on the inner surface was blown by air stream, before measuring the wet weight of the membrane. Then the membranes were further dried in a vacuum oven for 2 h at 120 ◦C, before measuring the dry weight. In order to assess the mechanical stability of the hollow fiber membranes, a collapsing pressure test was performed. During the gas permeation test, the upstream pressure on the shell side was increased at 0.5×10^5 Pa intervals. Collapsing pressure is the pressure at which a sudden change, either decrease or increase, in the permeate flow on the lumen side is observed.

2.6. CO_2 stripping experiment

The CO_2 stripping flux and efficiency of fabricated membranes was measured using a membrane contactor module. A total of 30 hollow fibers were packed randomly in a stainless steel membrane module. The details of the membrane contactor module are given in Table 2.

Table 2
Specifics of the gas-liquid membrane contactor.

Module i.d. (mm)	15
Module length (mm)	250
Fiber o.d. (mm)	0.9 to 1.0
Fiber i.d (mm)	0.45 to 0.50
Effective fiber length (mm)	180
Number of fibers	30

Pure nitrogen sweep gas flowed through the shell side while MEA solution (0.1 M) preloaded at room temperature with CO_2 by another membrane contactor flowed through the lumen side of the hollow fibers in a counter-current flow mode. The pressure and the flow rate of gas and liquid were controlled by the control valves. The liquid pressure was higher than gas pressure by 0.2×10^5 Pa to avoid the formation of bubbles on the liquid side [29]. The operating temperature and pressure were kept constant at 80 ◦C and 0.5×10^5 Pa, respectively, unless otherwise mentioned. The CO_2 concentrations in the liquid phase at the inlet and outlet of the stripper module were measured to determine stripping flux and efficiency by using the chemical titration method. Before collecting liquid samples, all the experiments were carried out for 30 min to achieve a steady state condition. Figure 1 shows the flow diagram of the experimental stripping membrane contactor system schematically. The CO_2 stripping efficiency (η) of the module was calculated as:

$$\eta(\%)=\left[1-\frac{C_{l,o}}{C_{l,i}}\right]\times100 \quad (5)$$

The experimental CO_2 stripping flux was calculated based on the inner surface of the hollow fibers as:

$$J_{CO_2}=\frac{(C_{l,i}-C_{l,o})\times Q_l}{A_i} \quad (6)$$

where J_{CO2} is the CO_2 stripping flux (mol/m^{2}s), Q_l is liquid flow rate (m^3/s), and A_i is inner surface of the hollow fiber membranes.

3. Results and discussion

3.1. Morphology of the hollow fiber membranes

The PEI hollow fiber membranes were fabricated using a wet spinning method with three different additive concentrations in the spinning solutions. The morphologies of the membranes were studied by FESEM to investigate the cross-section at different magnifications. The fabricated hollow fiber membranes have outer diameters ranging from 0.75 to 0.9 mm, inner diameters ranging from 0.40 to 0.45mm and wall thickness ranging from 0.175 to 0.225 mm.

The cross-sectional structure of the membranes is depicted in Figures 2(A)–(C). Figures 2(A)-(C) show that all the hollow fibers have a sublayer with finger-like macro-voids, originating from inner and outer surfaces of the hollow fiber and extending to the middle section of the hollow fiber wall. All the membranes exhibited a skinless inner surface. This is due to the high NMP content in the inner coagulant. In fact, this phenomenon resulted in open microporous structure in the inner surface. However, employing water as the external coagulant provided membranes with an outer skin layer, since water acts as a strong non-solvent.

3.2. Effect of the additives on the hollow fiber membrane structure

The results from the gas permeation experiments, CEPw measurement, porosity measurement and collapsing pressure are summarized in Table 3. Porosities are in the range of 74.24 to 76.50%, which are considered to be high enough and are ascribed to the low polymer concentration in the dope.

Figure 3 shows the N_2 permeance versus mean pressure. The data fit the straight line relationship with reasonably high correlation coefficients, R^2. These data were used to calculate the average pore size, according to the method shown in the experimental section and the results given in Table 3. It must be mentioned that the average pore size does not have any significant physical meaning, especially for the membranes prepared by phase-inversion processes. However, this can be used as a parameter which can be compared quantitatively for the membranes prepared under different spinning conditions [30]. As can be seen, N_2 permeances calculated for all the membranes tend to increase with an increase in mean pressure. Such a phenomenon indicates that both the Poiseuille and Knudsen flows govern the N_2 permeation through the PEI membranes. As the slope for the membrane prepared with 4 wt.% of ethanol as additive was very small, it indicates that Knudsen flow contributes to the gas permeation more than the Poiseuille flow due to small pore sizes. On the other hand, the slope for the membrane prepared with 2 wt.% ethanol was larger. It seems that the Poiseuille flow is dominant for this membrane due to the large pore sizes.

As for the critical entry pressure of water, all membranes can withstand the excess pressure applied on the shell side (0.2×10^5 Pa) during the CO_2 absorption process. The membrane fabricated with 4 wt.% ethanol in the spinning dope resulted in the lowest CEPw (see Table 3), which is associated with the largest average pore size.

3.3 Effect of the additives on the CO2 stripping performance

Figures 4 shows the effect of liquid velocity on the CO_2 stripping flux of fabricated membranes. As can be seen, CO_2 stripping flux increased by increasing liquid velocity. It was observed from Figure 2 that the CO_2 stripping fluxes of the membrane prepared with 4 wt. % of ethanol were significantly lower than the other membranes. The effective surface porosity of this membrane is smaller than the other membranes. Therefore, the contact area between gas and liquid is smaller and stripping flux is smaller than other membranes. With the membrane prepared with 2 wt.% ethanol as additive in the spinning dope, a maximum CO_2 flux was achieved at the liquid flow rate of 200 (ml/min) (= 0.7 m/s), which was almost more than the membrane prepared with 4 wt.% of ethanol as additive. As the membrane which was fabricated using 2 wt.% additive showed higher CO_2 stripping flux, in order to study the effect of operation conditions on stripping flux, this membrane was selected.

Figure 5 shows the effect of liquid velocity on the CO_2 stripping flux and CO_2 concentration in the outlet liquid. The effect of liquid velocity on the stripping efficiency is shown in Figure 5. As can be seen, stripping flux and stripping efficiency increased by increasing liquid velocity. The highest stripping flux of 2.09×10^{-4} (mol/m^{2}s) and the lowest CO_2 concentration in the outlet liquid of 1.2×10^{-4} (mol/l) were achieved at the liquid flow rate of 200 (ml/min) (= 0.7 m/s), respectively. The highest stripping efficiency of almost 80% was also achieved. This is due to the reduction in liquid boundary layer

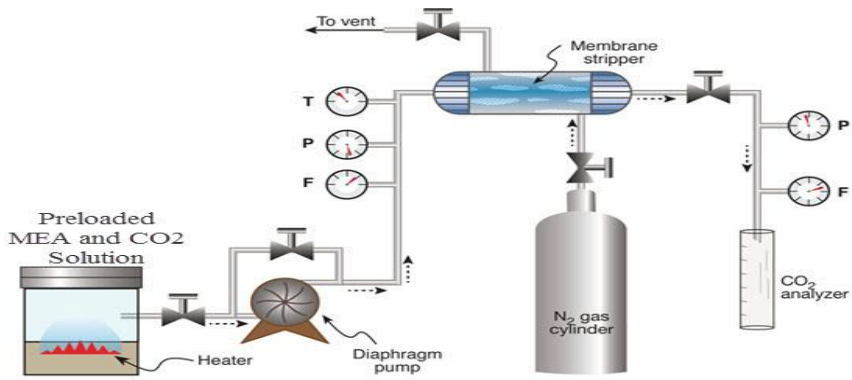

Fig.1. Flow diagram of experimental stripping membrane contactor system.

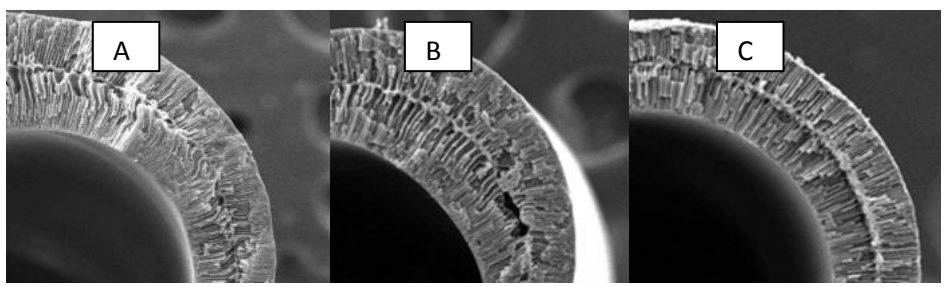

Fig. 2. FESEM micrograph of cross-sectional structure of the PEI hollow fiber membranes: (A) Without additive, (B) 2 wt.% ethanol, (C) 4 wt.% ethanol.

Table 3
Properties of fabricated PEI hollow fiber membranes.

Additive	Average pore size (nm)	Effective surface porosity ε/L_p (m^{-1})	CEPw ($\times 10^5$ Pa)	Overall porosity (%)	Collapsing pressure ($\times 10^5$ Pa)	Contact angle
Without additive	31.32	38.83	7	72.74	7.5±0.5	75.50
Ethanol (2 wt.%)	24.50	75.12	7.5	75.50	7±0.5	79.25
Ethanol (4wt.%)	35.46	25.39	6.5	73.24	8±0.5	72.25

resistance and the increase in CO_2 mass transfer coefficient at higher liquid flow rates [31]. On the other hand, Khaisri et al. [32] reported that the gas phase mass transfer resistance has a minor effect on the desorption performance of a CO_2 stripping membrane contactor system. According to them, the contribution of the gas phase mass transfer resistance to the overall mass transfer resistance is approximately 5–10%. Kumazawa [33] and Koonaphapdeelert et al. [34] found that the mass transfer in gas stripping membrane contactors was mainly controlled by the liquid film mass transfer coefficient. It can therefore be reasonably concluded that the liquid phase controls the overall mass transfer resistance of desorption processes by the membrane contactor. This trend was also similar to most gas absorption and stripping studies in membrane contactor applications [35-37].

As shown in Figure 5, the CO_2 concentration in the liquid outlet decreased considerably with an increase in liquid velocity. Therefore, a higher stripping flux and efficiency were achieved at higher liquid velocity (Figures 5 and 6).

3.4 Effect of gas velocity on CO2 stripping flux

The effect of gas velocity was examined at 80 ◦C rich solution temperature. The results in Figure 7 show that the enhancement of CO_2 stripping flux with gas velocity was not significant. The CO_2 desorption flux increased from 6.55×10^{-7} to 2.62×10^{-6} ($mol.m^{-2}.s^{-1}$) by increasing the gas flow rate from 50 to 200 ($ml.min^{-1}$). As can be seen, an increase in the gas velocity increased the CO_2 desorption flux but this change was negligible. The results confirmed the previous discussion that the liquid phase mass transfer resistance is the controlling resistance in the system.

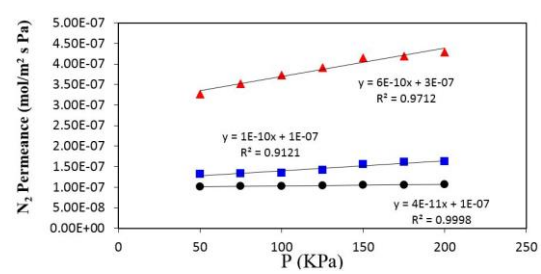

Fig.3. Measured N_2 permeance as a function of mean pressure for PEI hollow fiber membranes. (■ without additive, ▲PEI+2 wt.% Ethanol, ● PEI+4 wt.% Ethanol).

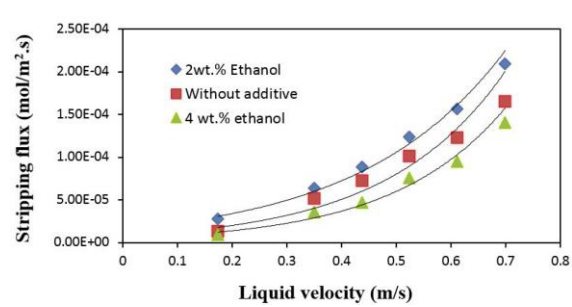

Fig. 4. Effect of the liquid velocity on CO_2 stripping flux and CO_2 concentration in outlet liquid.

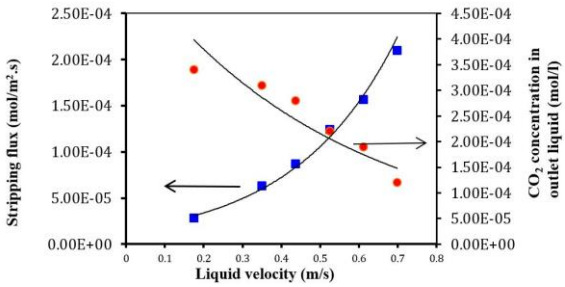

Fig. 5. Effect of liquid velocity on stripping efficiency.

Figure 8 shows experimental results for the effect of liquid phase temperature on CO_2 stripping flux through the membrane contactor module. As can be seen, the CO_2 stripping flux is significantly affected by the liquid phase temperature, which can be related to the decrease of CO_2 solubility with increasing temperature. At higher temperatures, CO_2 is dissolved in MEA solution at the equilibrium tends to be released to the gas phase, which results in the increase of driving force for mass transfer of CO_2. From Figure 8, when the liquid temperature increased from 80 to 90 ◦C, the CO_2 stripping flux increased from 2.1×10^{-4} to 5.1×10^{-4} mol.m^{-2}.s^{-1} at a liquid velocity of 200 ml.min-1 (=0.7 m.s^{-1}). As Figure 8 shows, the liquid phase temperature is a key parameter that needs to be controlled.

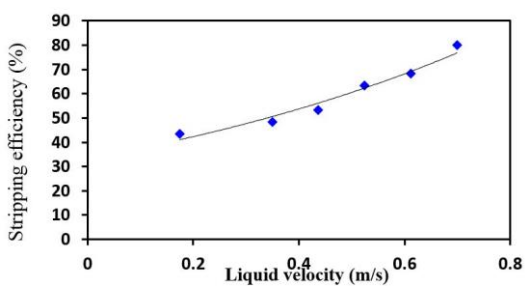

Fig. 6. Effect of gas velocity on CO_2 stripping flux.

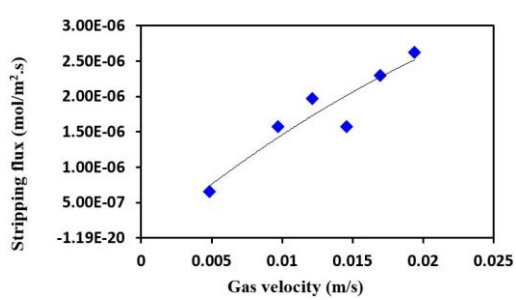

Fig. 7. Effect of liquid phase temperature on CO_2 stripping flux.

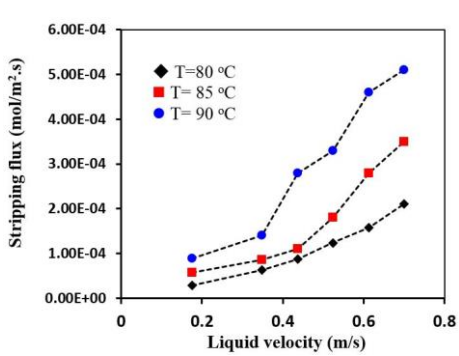

Fig. 8. Effect of liquid phase temperature on CO_2 stripping flux.

4. Conclusions

All the hollow fibers have a sublayer with finger-like macro-voids, originating from inner and outer surfaces of the hollow fiber and extending to the middle section of the hollow fiber wall. All the membranes exhibited a skinless inner surface. This is due to the high NMP content in the inner coagulant. Porosities are in the range of 74.24 to 76.50%, which are considered to be high enough and are ascribed to the low polymer concentration in the dope. As for the critical water entry pressure, all membranes can withstand the excess pressure applied on the shell side during the CO_2 absorption process. Stripping flux and stripping efficiency increased by increasing liquid velocity. The highest stripping efficiency of almost 80% was also achieved. This is due to the reduction in liquid boundary layer resistance and the increase in CO_2 mass transfer coefficient at higher liquid flow rates. The CO_2 concentration in the liquid outlet decreased considerably with an increase in liquid velocity. Therefore, higher stripping flux and efficiency were achieved at higher liquid velocity. An increase in the gas velocity increased the CO_2 desorption flux but this change was negligible. The results confirmed the previous discussion that the liquid phase mass transfer resistance is the controlling resistance in the system. When the liquid temperature increased from 80 to 90 ◦C, the CO_2 stripping flux increased. Thus, the liquid phase temperature is a key parameter that needs to be controlled.

Nomenclature

CO_2 stripping flux: mol/m^{2}s (J_{CO2})
Effective pore length: m (L_p)
Gas constant: 8.314 J/mol.K (R)
Gas molecular weight: kg/mol (M)
Gas permeance: mol/m^{2}sPa (J_i)
Gas temperature: K (T)
Gas viscosity: kg/m.s (μ_i)
Inner surface of the hollow fiber membranes: m^2 (A_i)
Liquid flow rate: m^3/s (Q_l)
Liquid phase CO_2 concentration intlet: mol/m^3 ($C_{l,i}$)
Liquid phase CO_2 concentration outlet: mol/m^3 ($C_{l,o}$)
Mean pressure: Pa (P)
Pore radius: m (r_p)
Surface porosity: ε

References

[1] F.A. Tobiesen, H.F. Svendsen, Study of a modified amine-based regeneration unit, Ind. Eng. Chem. Res. 45 (2006) 2489–2496.
[2] G.W. Xu, C.F. Zhang, S.J. Qin, B.C. Zhu, Desorption of CO2 from MDEA and activated MDEA solutions, Ind. Eng. Chem. Res. 34 (1995) 874–880.
[3] S. Khaisri, D. deMontigny, P. Tontiwachwuthikul, R. Jiraratananon, Comparing membrane resistance and absorption performance of three different membranes in a gas absorption membrane contactor, Sep. Purif. Technol. 65 (2009) 290–297.
[4] D. deMontigny, P. Tontiwachwuthikul, A. Chakma, Comparing the absorption performance of packed columns and membrane contactors, Ind. Eng. Chem. Res. 44 (2005) 5726–5732.
[5] G. Bakeri, A.F. Ismail, M. Shariaty-Niassar, T. Matsuura, Effect of polymer concentration on the structure and performance of polyetherimide hollow fiber membranes, J. Membr. Sci. 363 (2010)103–111.
[6] K.C. Khulbe, C.Y. Feng, F. Hamad, T. Matsuura, M. Khayet, Structural and performance study of micro porous polyetherimide hollow fiber membranes prepared at different air-gap, J. Membr. Sci. 245 (2004)191–198.
[7] Z.-K. Xu, L.-Q. Shen, Q. Yang, F. Liu, S.-Y. Wang, Y.-Y. Xu, Ultrafiltration hollow fiber membranes from poly(etherimide):preparation, morphologies and properties, J. Membr. Sci. 223 (2003)105–118.
[8] K. Kneifel, K.-V. Peinemann, Preparation of hollow fiber membranes from polyetherimide for gas separation, J. Membr. Sci. 65 (1992)295–307.
[9] D. Wang, K. Li, W.K. Teo, Preparation and characterization of polyetherimide asymmetric hollow fibermembranes for gas separation, J. Membr. Sci. 138 (1998) 193–201.
[10] G. Bakeri, T. Matsuura, A.F. Ismail, The effect of phase inversion promoters on the structure and performance of polyetherimide hollow fibermembrane using in gas–liquid contacting process, J. Membr. Sci. 383 (2011)159–169.
[11] A.J. Reuvers, C.A. Smolders, Formation of membranes by means of immersion precipitation. Part II. The mechanism of formation of membranes prepared from the system CA/acetone/water, J. Membr. Sci. 34 (1987) 67–86.
[12] R.E. Kesting, Synthetic Polymeric Membranes, McGraw-Hill, New York, NY, 1991.
[13] M.J. Han, S.T. Nam, Thermodynamic and rheological variation in Polysulfone solution by PVP and its effect in the preparation of phase inversion membrane, J. Membr. Sci. 202 (2002) 55–61.
[14] A.F. Ismail, A.R. Hassan, Effect of additive contents on the performances and structural properties of asymmetric polyethersulfone (PES) nanofiltration membranes, Sep. Purif. Technol. 55 (2007) 98–109.

[15] Y. Liu, G.H. Koops, H. Strathmann, Characterization of morphology controlled polyethersulfone hollow fiber membranes by the addition of polyethylene glycol to the dope and bore liquid solution, J. Membr. Sci. 223 (2003) 187–199.
[16] S. Atchariyawut, C. Feng, R. Wang, R. Jiraratananon, D.T. Liang, Effect of membrane structure on mass-transfer in the membrane gas–liquid contacting process using microporous PVDF hollow fibers, J. Membr. Sci. 285 (2006) 272– 281.
[17] Z.L. Xu, F.A. Qusay, Polyethersulfone (PES) hollow fiber ultrafiltration membranes prepared by PES/non-solvent/NMP solution, J. Membr. Sci. 233 (2004) 101–111.
[18] C. Stropnik, V. Kaiser, V. Musil, M. Brumen, Wet-phase-separation membranes from the polysulfone/N,N-dimethylacetamide/water ternary system: the formation and elements of their structure and properties, J. Appl. Polym. Sci. 96 (2005) 1667–1674.
[19] D. Wang, K. Li, W.K. Teo, Porous PVDF asymmetric hollow fiber membranes prepared with the use of small molecular additives, J. Membr. Sci. 178 (2000) 13–23.
[20] A. Xu, A. Yang, S. Young, D. deMontigny, P. Tontiwachwuthikul, Effect of internal coagulant on effectiveness of polyvinylidene fluoride membrane for carbon dioxide separation and absorption, J. Membr. Sci. 311 (2008) 153–158.
[21] S.P. Deshmukh, K. Li, Effect of ethanol composition in water coagulation bath on morphology of PVDF hollow fiber membranes, J. Membr. Sci. 150 (1998) 75–85.
[22] D. Wang, W.K. Teo, K. Li, Preparation and characterization of high-flux polysulfone hollow fiber gas separation membranes, J. Membr. Sci. 204 (2002) 247–256.
[23] M. Rahbari-Sisakht, A.F. Ismail, D. Rana, T. Matsuura, D. Emadzadeh, Carbon dioxide stripping from water through porous polysulfone hollow fiber membrane contactor, Sep. Purif. Technol. 108 (2013) 119–123.
[24] A. Mansourizadeh, A.F. Ismail, Effect of additives on the structure and performance of polysulfone hollow fiber membranes for CO2 absorption, J. Membr. Sci. 348 (2010) 260–267.
[25] A.F. Ismail, A.R. Hassan, Effect of additive contents on the performances and structural properties of asymmetric polyethersulfone (PES) nanofiltration membranes, Sep. Purif. Technol. 55 (2007) 98–109.
[26] P. Luis, B. Van der Bruggen, T. Van Gerven, Non-dispersive absorption for CO2 capture:from the laboratory to industry, J. Chem. Technol. Biotechnol. 86 (2011) 769–775.
[27] M.J. Han, S.T. Nam, Thermodynamic and rheological variation in polysulfone solution by PVP and its effect in the preparation of phase inversion membrane, J. Membr. Sci. 202 (2002) 55–61.
[28] Li K, Kong JF, Wang D,Teo WK. Tailor-made asymmetric PVDF hollow fiber for soluble gas removal, AIChE J. 45 (1999) 1211–1219.
[29] M. Mavroudi, S.P. Kaldis, G.P. Sakellaropoulos, Reduction of CO2 emissions by a membrane contacting process, Fuel 82 (2003) 2153–2159.
[30] H.C. Shih, Y.S. Yeh, H. Yasuda, Morphology of microporous poly(vinylidene fluoride) membranes studied by gas permeation and scanning microscopy, J.Membr. Sci. 50 (1990) 299–317.
[31] S.-H, Choi, F. Tasselli, J.C. Jansen, G. Barbieri, E. Drioli, Effect of the preparation conditions on the formation of asymmetric poly(vinylidene fluoride) hollow fibre membranes with a dense skin. Eur. Polym. J. 46 (2010) 1713–1725.
[32] S. Khaisri, D. deMontigny, P. Tontiwachwuthikul, R. Jiraratananon, CO2 stripping from monoethanolamine using a membrane contactor. J. Membr. Sci. 376 (2011) 110–118.
[33] H. Kumazawa, Absorption and desorption of CO2 by aqueous solutions of sterically hindered 2-amino-2-methyl-1-propanol in hydrophobic microporous hollow fiber contained contactors. Chem. Eng. Commun. 182 (2000) 163–179.
[34] S. Koonaphapdeelert, Z. Wu, K. Li, Carbon dioxide stripping in ceramic hollow fiber membrane contactors, Chem. Eng. Sci. 64 (2009) 1–8.
[35] M. Rahbari-Sisakht, D. Rana, T. Matsuura, D. Emadzadeh, M. Padaki, A.F. Ismail, Study on CO2 stripping from water through novel surface modified PVDF hollow fiber membrane contactor, Chem. Eng. J. 246 (2014) 306–310.
[36] M. Rahbari-Sisakht, A.F. Ismail, D. Rana, T. Matsuura, Effect of different additives on the physical and chemical CO2 absorption in polyetherimide hollow fiber membrane contactor system, Sep. Purif. Technol. 98 (2012) 4.
[37] M. Rahbari-Sisakht, A.F. Ismail, D. Rana, T. Matsuura, Effect of novel surface modifying macromolecules on morphology and performance of Polysulfone hollow fiber membrane contactor for CO2 absorption, Sep. Purif. Technol. 99 (2012) 61–68.